Characteristics of long-lived persistent spectral holes in Eu³⁺:Y₂SiO₅ at 1.2 K

René Oswald, Michael G. Hansen, Eugen Wiens, Alexander Yu. Nevsky, and Stephan Schiller[*]

Institut für Experimentalphysik, Heinrich-Heine-Universität Düsseldorf, 40225 Düsseldorf, Germany

Properties of persistent spectral holes (SHs) relevant for frequency metrology have been investigated in the system $Eu^{3+} : Y_2SiO_5$ (0.5%) at crystallographic site 1 and a temperature of 1.2 K. Hole linewidths as small as 0.6 kHz have been reliably achieved. The theoretically predicted T^4 dependence of the frequency shift with temperature has been confirmed with high precision. The thermal hysteresis of the SH frequency between 1.15 and 4.1 K was measured to be less than 6×10^{-3} fractionally. After initially burning a large ensemble of SHs, their properties were studied on long time scales by probing different subsets at different times. SHs could still be observed 49 days after burning if not interrogated in the meantime. During this time, the SH linewidth increased by 1.5 kHz, and the absorption contrast decreased from 35% to 15%. During a 14-day interval the absolute optical frequencies of previously unperturbed spectral holes were measured with respect to a Global-Positioning-System-monitored active H maser, using a femtosecond frequency comb. The fractional frequency drift rate exhibited an upper limit of 2.3×10^{-19} s^{-1}, 65 times smaller than the most stringent previous limit.

I. INTRODUCTION

Recent progress in the performance of optical clocks, based on cold-atom ensembles or single ions [1–4], has become possible due to a strong improvement of the short-term frequency stability of the "clock" lasers that interrogate the atomic transitions [5,6]. Today's clock lasers are realized by using macroscopic solid-state references, high-finesse optical cavities. Ultimately, the frequency stability of a clock laser corresponds to the stability of the cavity's length. The latter is fundamentally limited by thermal noise and often also by vibrations induced by environmental noise. Nevertheless, excellent frequency instabilities have been reached, with the lowest values currently at 4×10^{-17} fractionally [7]. As of today, only very few approaches have been identified that have the potential of surpassing the resonator approach [8].

One solution is the use of persistent spectral holes in rare-earth-doped crystals at cryogenic temperatures. Here, a large ensemble of atomic ions ($\simeq 10^{20}$) is embedded in a crystalline host; on the order of 10^{14} ions contribute to a single spectral hole (SH) and provide a narrow-linewidth frequency reference. This approach, suggested already more than two decades ago [9–13], combines advantageous features of atomic and macroscopic solid-state references.

The first report of frequency stabilization of a laser to an SH, using the Pound-Drever-Hall technique, dates back to 1999 [11]. A complication in this approach is that an SH is not a "static" reference but is modified dynamically by the interrogating laser field [14], a fact that must be taken into account in the experimental scheme. More recent work showed that SHs with narrow, kHz-level linewidths persist for times up to weeks with a high signal contrast [15]. In order to minimize the modification of the SHs by the laser radiation

to be stabilized, Cook *et al.* [16] have developed a technique that uses a pattern of hundreds of SHs for frequency stabilization. An excellent frequency instability at the 1×10^{-16} fractional level was thereby achieved for a 580-nm laser resonant with the $F_0 \rightarrow D_0$ transition of the $Eu^+ : Y_2SiO_5$ system at 580 nm. Recently, in the same system, a heterodyne detection technique for laser frequency locking to a single spectral hole was demonstrated [17]. Both techniques allow continuous (uninterrupted) frequency stabilization of a laser.

The long-term frequency stability of an SH on timescales of minutes and longer and therefore its utility for long-term frequency stabilization of lasers or for potential studies of fundamental physics depends also on systematic effects caused by external disturbances. Disturbances such as variations of temperature and of magnetic field, and also energy exchange on the atomic scale, result in SH frequency shift, SH contrast decrease and SH linewidth increase over time. These issues have been studied in detail in the system $Eu^+ : Y_2SiO_5$ at 4 K [15,16,18] and at 3 K [19], including accurate determinations of the temperature dependence of the SH frequency. To minimize the influence of this latter effect, Thorpe *et al.* [15] implemented a compensation system making use of the dependence of SH frequency on gas pressure.

In laser frequency stabilization on long time intervals, an extreme case is the time scale of days and weeks after burning SHs. On this time scale the drift of the SH frequency and the modification of the SH line shape was first investigated in Ref. [19]. A drift consistent with 0 ($<1.5 \times 10^{-17}$/s at 1σ level) was observed at 3 K, which was later confirmed in Ref. [20]. In this paper we extend the study of the long–term properties of persistent SHs to lower temperature, near 1.2 K. This is one of the lowest temperatures used so far in SH studies. One particular aspect of our approach was to probe the spectral holes cautiously. For example, SHs were left unperturbed spectrally for up to 49 days until interrogation occurred and then interrogated only once by a single absorption scan.

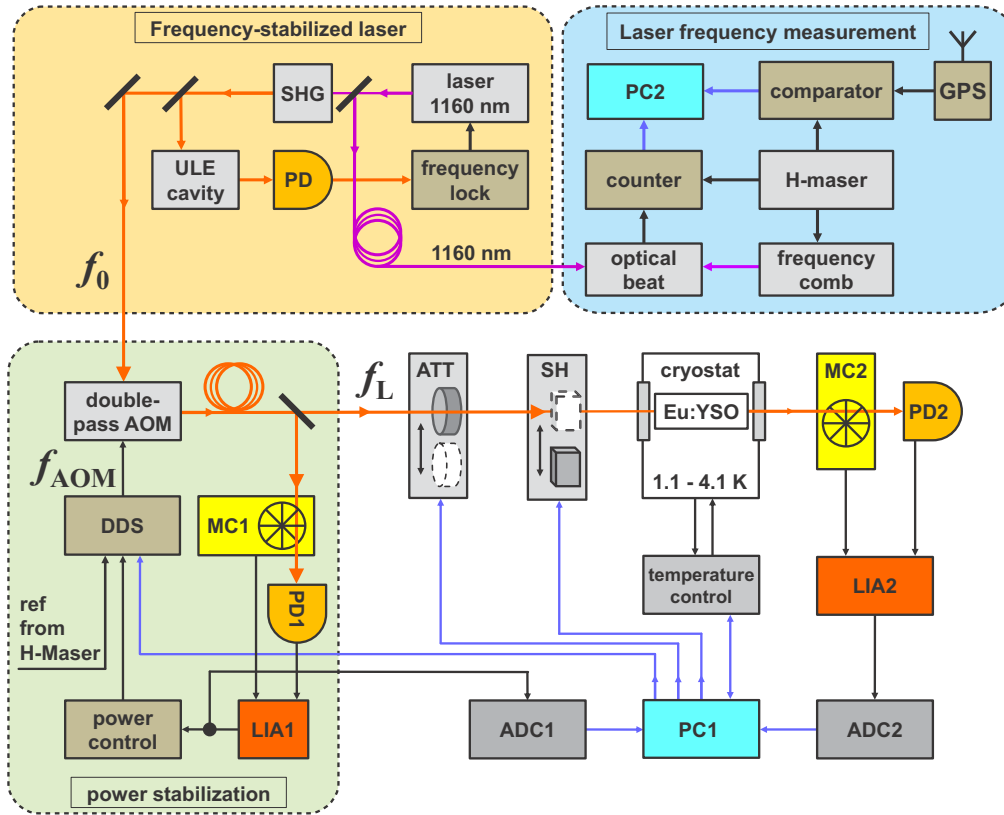*step.schiller@hhu.de; http://www.exphy.uni-duesseldorf.de/

FIG. 1. Experimental setup. PD, photo detector; SHG, second harmonic generation; ULE, high-finesse ultralow thermal expansion glass optical cavity,; AOM, acusto-optic modulator; DDS, direct digital synthesizer; MC, mechanical chopper; LIA, lock-in amplifier; ATT, attenuator; SH, shutter; ADC, analog-to-digital converter; and PC, personal computer.

II. EXPERIMENT

Absorption spectroscopy experiments were carried out on the $^7F_0 \rightarrow {}^5D_0$ transition of Eu$^+$ ions of the crystallographic site 1 in a Y$_2$SiO$_5$ host crystal [9], in the temperature range of 1.15 – 4.1 K. A schematic of the experimental setup is shown in Fig. 1.

The Eu$^+$: Y$_2$SiO$_5$ crystal with 0.5% rare-earth ion concentration has dimensions of $5 \times 5.5 \times 10$ mm^3, with the polished 5×5.5 mm^2 facets parallel to the $D1$ and $D2$ axes. The crystal was placed inside a ring-shaped rare-earth permanent magnet with a maximum magnetic field of approximately 0.8 T. The crystal and the magnet were mounted on a copper plate inside the cryostat. A closed-cycle pulse-tube cooler cryostat equipped with a Joule-Thomson stage was used for cooling. This allowed crystal temperatures as low as 1.15 K to be achieved.

For burning and interrogating SHs we used an external-cavity diode laser stabilized to a high-finesse ULE optical resonator. A description of this system, operating at 1156 nm, is given in Ref. [21]. In the present experiment, with the laser operating at 1160 nm, the linewidth was approximately 50 Hz. The radiation was frequency doubled to 580 nm, led to the cryostat using a 5-m-long polarization-maintaining optical fiber, and focused into the crystal using a fiber collimator. The beam diameter in the focus was 300 µm. The light transmitted through the crystal was detected with a low-noise silicon

photodetector (PD2). A remotely controlled attenuator, based on a neutral density filter and a mechanical shutter were used to control the duration and laser power of the SH burning and read-out phases.

Before entering the cryostat, the laser light passed a beam splitter which deflected 30% of the radiation to a reference Si photodetector (PD1). Its signal was used for active stabilization of the laser power entering the crystal. To this end, an analog servo regulated the amplitude of the radio-frequency driver of an acusto-optic modulator (AOM). In addition, during the spectroscopy experiments, the output of PD1 was used for normalization of the value of the transmitted laser power, so as to reduce the influence of the laser power fluctuations on the measurements. The laser waves reaching the photodetectors PD1 and PD2 were modulated with chopper wheels (MC1 and MC2) at frequencies of 600 and 650 Hz, respectively. The photodetector signals were demodulated by respective lock-in amplifiers (LIA1 and LIA2). A typical lock-in integration time constant was 0.3 s. The output signals of both lock-in amplifiers were read out with a 10-bit analog-to-digital converter.

To tune the laser frequency, we used the AOM in a double-pass configuration driven by a computer-controlled DDS. It was referenced to a 10-MHz reference signal coming from an active hydrogen maser. The complete experiment including the DDS, the choppers, lock-in detectors, etc., was computer-

controlled with a LabVIEW program. The absolute frequency f_L of the wave interrogating the Eu^+ ions at 580 nm is determined by the stabilized, but slowly drifting, laser frequency at 580 nm, f_0, plus the total frequency shift introduced by the AOM, $f_L = f_0 + 2 f_{AOM}$.

The laser frequency was measured at 1160 nm ($f_0/2$) relative to the frequency of the active hydrogen maser, using a commercial erbium-doped fiber laser-based frequency comb (FC), optically stabilized to a home-built ULE-cavity-stabilized 1562-nm laser system by controlling the FC repetition rate. To this end, a fraction of the $f_0/2$ laser radiation was led to the comb laboratory via a 150-m-long unstabilized fiber. The heterodyne beat signal of the laser with a comb mode was measured with a dead-time-free frequency counter. The laser frequency $f_0/2$ was then evaluated in a conventional way from the beat frequency, the repetition rate, and the carrier envelope offset frequency. All respective counters were referenced to the maser. In addition, the maser's long-term frequency drift was monitored by a Global Positioning System (GPS) receiver.

III. SPECTRAL HOLES

A basic investigation consisted of the determination of conditions under which the burning produced SHs of appreciable strength but still having a narrow linewidth. To this end, we measured the dependence of the SH linewidth and the SH contrast on the burn phase duration. We define the SH contrast as $C_h = [S_{PD2}(\Delta = 0) - S_{PD2}(|\Delta| \gg FWHM)]/S_{PD2,max}$, where $S_{PD2}(\Delta)$ is the laser power measured by the transmission detector PD2 for a given interrogation laser detuning from the SH line center, Δ. $S_{PD2,max}$ is the power detected on-resonance for a "deeply" burnt SH, the crystal then being essentially transparent. FWHM denotes the full width at half maximum.

Different sets of five SHs with a frequency spacing of 20 kHz were burned with a laser power of 1.7 nW for durations from 10 to 320 s. Spectroscopy of the holes was carried out by tuning the frequency f_L in steps of 100 Hz within a ± 10 kHz frequency range around the SH center frequencies with a dwell time of 0.7 s per frequency value. For these measurements the laser power was reduced to 0.86 nW. The transmission data taken during such scans were fitted with Lorentzians and the FWHM linewidth values were determined. The mean FWHM values of five-hole sets are presented in Fig. 2(a). The SH linewidth dependence on burn duration was found to be approximately linear, with a slope of $s = 0.10$ kHz/min. For burn durations up to 150 s, the SH contrast [Fig. 2(b)] follows a linear dependence with a slope of 25%/min. At 320 s burn duration we observed a strong saturation effect.

We investigated the operational parameters for obtaining minimum SH linewidths. For example, we produced SHs with the same burn power level of 1.7 nW and a short burn time of 7 s. The parameters for the subsequent interrogation scan were optimized to obtain a high signal-to-noise ratio. The frequency of the interrogation wave was stepped in 100-Hz increments every 0.5 s. The SH spectra obtained are shown in Fig. 3. The mean FWHM linewidth is 0.61(7) kHz. This should be compared to the minimum possible value, the homogeneous
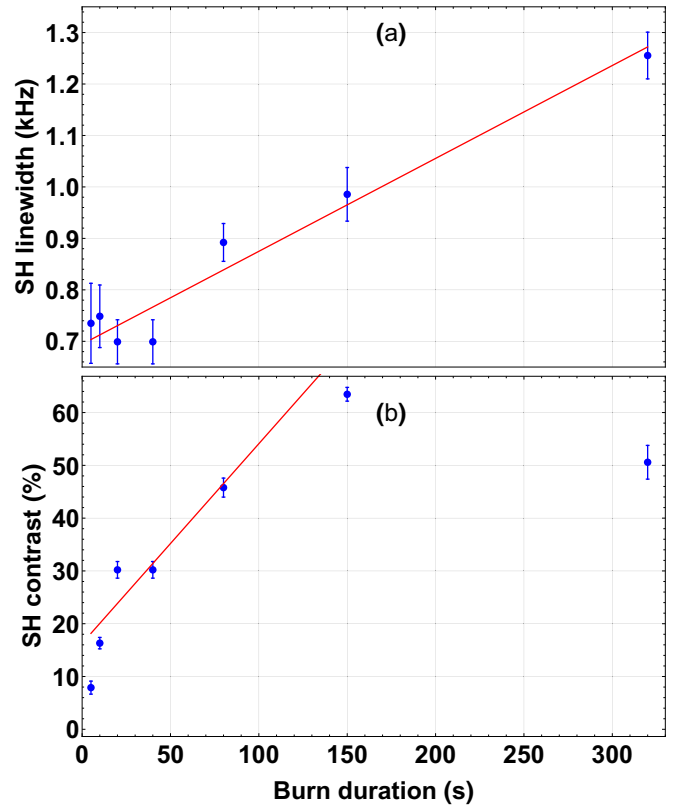

FIG. 2. (a) FWHM linewidths of spectral holes as a function of the burn time. Burn power is 1.7 nW; beam diameter is 300 μm. (b) Contrast C_h of the SHs, for different burn times.

linewidth of the SHs, $\Gamma_{hom,min} = 122$ Hz, derived from photon echo decay measurements [22,23]. We note that even for our comparatively low linewidth value, the signal contrast is still appreciable. For example, for the spectral hole 1 in Fig. 3, it was 15%. Further reduction of the burning laser power and of the interrogation time did not allow us to obtain narrower linewidths.
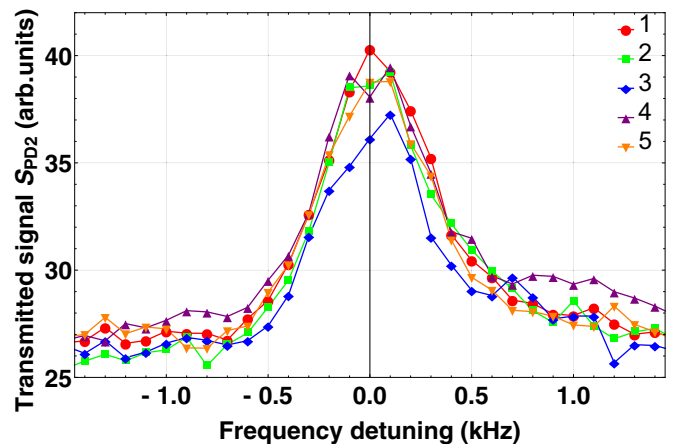

FIG. 3. Transmission signals of five different SHs exhibiting the smallest observed linewidths. The frequency scales for each hole were shifted so as to overlap the peaks. The measurement conditions are described in the text.
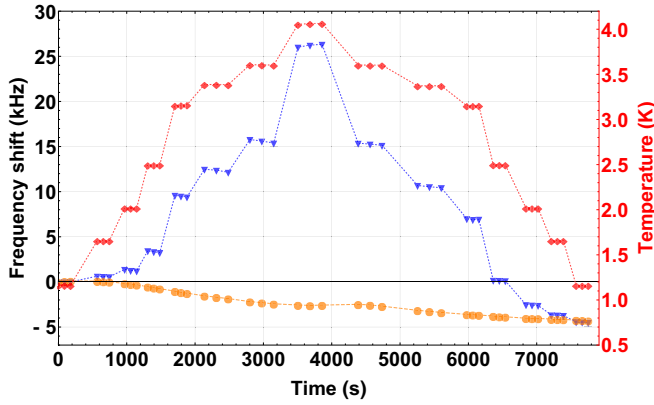
FIG. 4. Variation of the SH center frequencies as found from the AOM frequency shift $2\,\Delta f_{\mathrm{AOM},j}(t)$ (blue triangles) as the crystal temperature (red diamonds) is increased from 1.15 to 4 K and cooled back again. The independently occurring drift of the frequency-doubled laser frequency, $\Delta f_0(t)$, is shown as orange circles. Each blue point corresponds to one scan over one SH.

IV. TEMPERATURE-INDUCED FREQUENCY SHIFTS AND THERMAL HYSTERESIS

The temperature-induced shift of the SH center frequency was measured previously by Könz *et al.* [24] in the range of 4 to 320 K for sites 1 and 2, and a discussion of the underlying physics was given. A precise measurement was performed by Chen *et al.* [19] in the range of 3 to 4 K for site 1 and by Thorpe *et al.* for sites 1 and 2 in the ranges 2.2 to 8.5 K [15] and 2.5 to 5.5 K [18]. In the present experiment we measured the site 1 shift in the range of 1.15 to 4.1 K. The determination of the shift at the lower end of this range is challenging, due to its drop-off according to an expected T^4 dependence.

The frequency shift upon temperature cycling was studied by Chen *et al.* [19]. No effect was observed at the few kilohertz level. Here we set a more precise upper limit.

A. Procedures

After starting the laser frequency ($f_0/2$) measurement, 66 SHs were burnt at 1.15 K, spaced by $\delta f_{\mathrm{L}} = 100\,\mathrm{kHz}$. The burning time was set to 2 s and the laser power to 26 nW. The hole-burning procedure had a total duration of about 8 min. During the burn phase the laser frequency exhibited a nonlinear drift. Its time dependence was therefore fitted by a nonlinear function. By this procedure we assigned a center frequency, $f_{\mathrm{SH},j}^{\mathrm{burn}} = f_{\mathrm{SH}}(t_j^{\mathrm{burn}})$, to every SH j created at a particular time, t_j^{burn}. The typical uncertainty was $\sigma_{f_{\mathrm{L}},\mathrm{burn}} = 60\,\mathrm{Hz}$.

Over the course of 1 h, the temperature was increased to 4.1 K in steps of several 0.1 K and afterwards decreased again (see Fig. 4, red diamonds). After each step, at constant temperature, three so far not interrogated SHs were scanned and the mean of their center frequencies was determined. For this SH spectroscopy, the laser power was reduced by a factor of 10 and the AOM frequency was changed in steps of 100 Hz with a dwell time of 0.7 s. The recorded data were fitted assuming a Lorentzian line shape, determining f_{fit}, and introducing an error σ_{fit} of about 10 Hz.
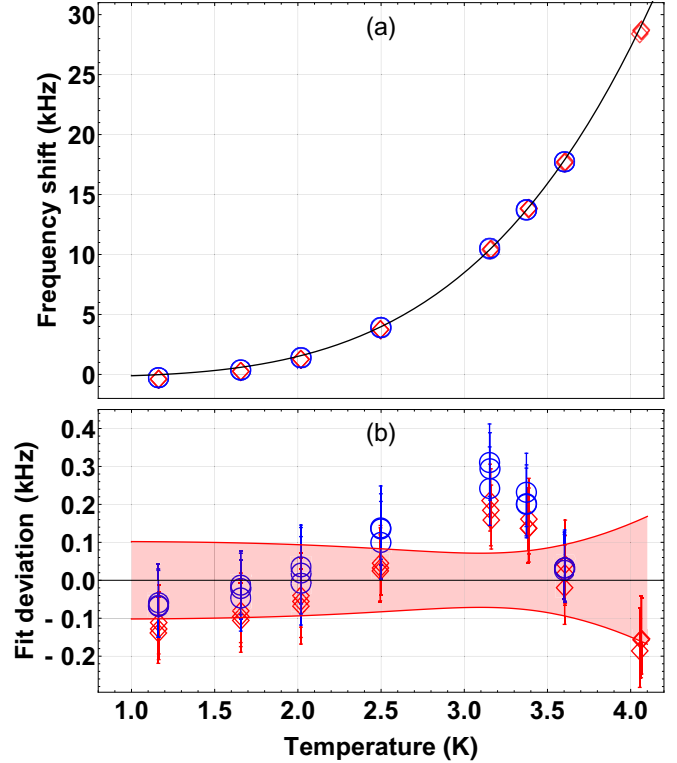

FIG. 5. Temperature dependence of the SH center frequencies for rising (red diamonds) and falling (blue circles) temperature. The black line in the upper graph is a fit to the model function $A\,T^4 + B$. Panel (b) shows the deviations from the fit and the $\pm 1\sigma$ fit uncertainty interval.

The frequency of the laser during the spectroscopy was evaluated at the time instant when the SH center was reached, using a nonlinear fit as above. This resulted in the SH frequency $f_{\mathrm{SH},j}^{\mathrm{scan}}$. Its uncertainty arises from σ_{fit} and from the error of the FC measurement $\sigma_{f_{\mathrm{L}},\mathrm{scan}}$. Finally, the frequency shift of an SH j is $\Delta f_{\mathrm{SH},j} = f_{\mathrm{SH},j}^{\mathrm{scan}} - f_{\mathrm{SH},j}^{\mathrm{burn}}$. We assigned to it the uncertainty $\sigma_{\mathrm{shift}} = \sqrt{\sigma_{f_{\mathrm{L}},\mathrm{burn}}^2 + \sigma_{f_{\mathrm{L}},\mathrm{scan}}^2 + \sigma_{\mathrm{fit}}^2}$. A typical value was 90 Hz.

An overview of the recorded data is presented in Fig. 4. As a function of time it shows the temperature measured at the crystal, the drift of the frequency-doubled laser frequency $\Delta f_0(t)$ and $2\,\Delta f_{\mathrm{AOM},j}(t)$, the difference of the frequency offsets produced by the AOM at the observation time t and at the burning time.

B. Thermal frequency shift

The frequency shift data are shown as a function of temperature in Fig. 5(a). A theoretical model of the SH shift predicts a T^4 dependence, caused by a two-phonon Raman process affecting the impurity ions [9,24,25]. Our data were therefore fitted with the function $A\,T^4 + B$. This resulted in an accurate description of the data, and small residuals, see Figs. 5(a) and 5(b), with $A = 108(0.3)\,\mathrm{Hz/K^4}$ and $B = -216(37)\,\mathrm{Hz}$. Note that because of the small hysteresis (see Sec. IV C) we take into account the data for both rising and falling temperatures. In the work of Könz *et al.* [24] a value of $A' = 166(10)\,\mathrm{Hz/K^4}$
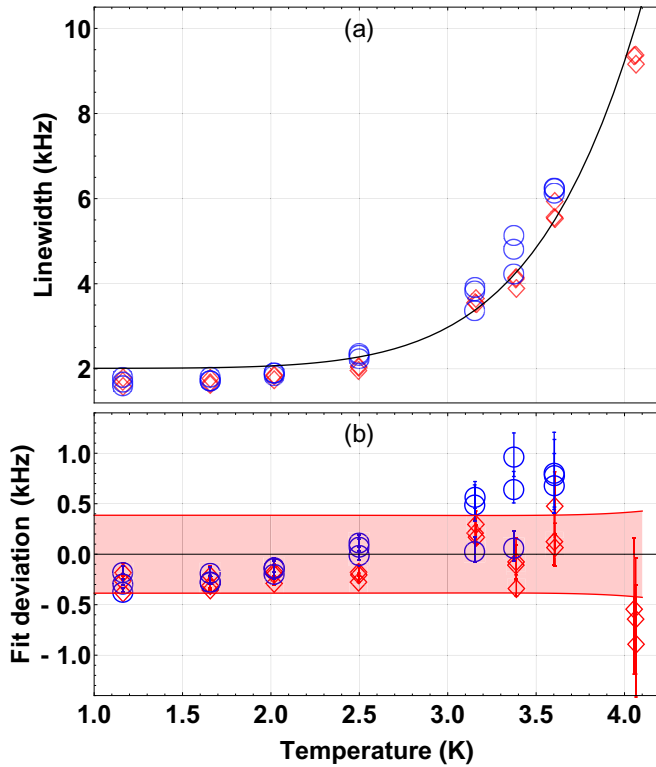
FIG. 6. Temperature dependence of the SH linewidth for rising (red diamonds) and falling (blue circles) temperature. The black line in panel (a) is a fit to the model function $C\,T^7 + D$. Panel (b) shows the deviations from the fit and the $\pm 1\sigma$ fit uncertainty interval.

has been found for the temperature-induced shift of site 1-ions. However, only values above 70 K were considered in the determination of the coefficient.

Our coefficient A also differs from the value $76(15)\,\mathrm{Hz/K^4}$ (for site 1) measured previously by Thorpe *et al.* [18]. As shown in that work the application of external pressure on the crystal through helium gas induces a linear frequency shift countering the effect of the temperature-induced frequency shift. This could explain the lower coefficient. Figure 6 shows the temperature dependence of the SH linewidth. The theoretical model [24,25] predicts a dependence of the type $C\,T^7 + D$. A fit of this function to our data yields $C = 0.44(2)\,\mathrm{Hz/K^7}$.

The value differs significantly from the value found by Könz *et al.* [24], $7.2 \times 10^{-4}\,\mathrm{Hz/K^7}$. However, their value was obtained from photon-echo-decay measurements. That method differs from our method: the photon echoes were measured on a timescale of microseconds, whereas our measurements were on the timescale of minutes (the typical duration of a frequency scan over a SH linewidth).

C. Thermal hysteresis

In Fig. 4 the AOM-induced frequency shift and the independently measured laser frequency drift rejoin at the end of the temperature cycle. Correspondingly, the red and blue data points at $T = 1.15\,\mathrm{K}$ in Fig. 5(a,b) nearly coincide. This shows that the thermal hysteresis of the SH frequencies is very small. More precisely, the residual shift upon returning
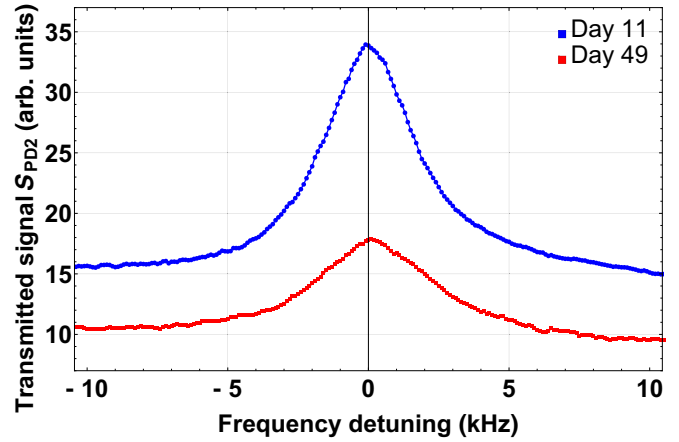

FIG. 7. Typical spectral holes observed during the long-term drift measurement. The upper blue points show a scan of a spectral hole 11 days after burning. The lower red points show another SH scanned 49 days after burning. In order to illustrate the typical deformation of the SHs, the respective frequency scales were shifted so as to center the peaks.

to the initial temperature was $\delta f_{\mathrm{hyst}} = 59\,\mathrm{Hz}$, which is within the measurement error σ_{shift}. Relating the sum of δf_{hyst} and σ_{shift} to the maximum frequency shift of 27 kHz at $T = 4\,\mathrm{K}$ allows us to state an upper limit of 6×10^{-3} for the fractional hysteresis.

V. LONG-TERM FREQUENCY DRIFT MEASUREMENT

A. Properties of long-lived spectral holes

In order to probe in a careful way the intrinsic long-term stability of the frequency of persistent SHs, we modified the experimental protocol compared to our previous work [19] in two significant aspects: (i) operation at significantly lower temperature, 1.15 K, and (ii) not performing multiple read-outs of the same SH. Our procedure consisted of initially burning a sufficiently large "reservoir" of 200 SHs with a frequency spacing of $\delta f_{\mathrm{L}} = 200\,\mathrm{kHz}$. The burn duration was set to 2 s with a relatively high laser power of 86 nW. The hole-burning procedure had a total duration of about 15 min. For the SH spectroscopy, the laser power was reduced by a factor of 10 and the AOM frequency was changed in steps of 100 Hz with a dwell time of 0.7 s per frequency value.

A typical line scan obtained under such conditions is shown in Fig. 7. During the scan the laser frequency was measured by the FC. The determination of the SH frequency shift $\Delta f_{\mathrm{SH},j}$ from $f_{\mathrm{SH},j}^{\mathrm{scan}}$, $f_{\mathrm{SH},j}^{\mathrm{burn}}$ and the measurement errors $\sigma_{f_{\mathrm{L,burn}}}$, $\sigma_{f_{\mathrm{L,scan}}}$, and σ_{fit} were obtained in the same fashion as described in Sec. IV.

Several times per week, over a period of 49 days, a subset of new (previously not interrogated) SHs was scanned. At the same time, the laser frequency was measured with the FC. Figure 8 shows an example of the result obtained on a particular day. The long-term variations of the SHs linewidths and contrasts are presented in Fig. 9. After 49 days we observed an increase of the linewidth by about 35%. The $1/e$ SH lifetime, extrapolated from the contrast decrease, is 50
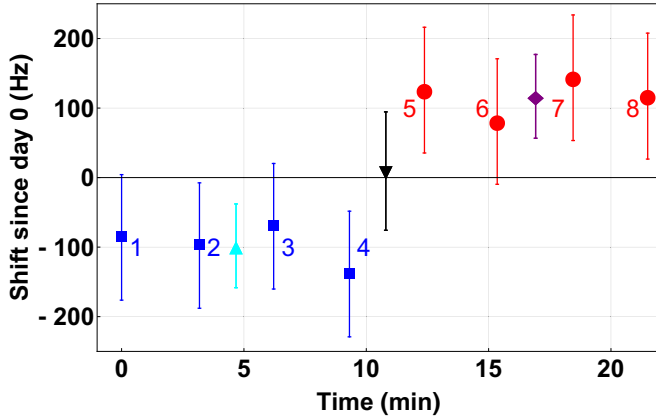
FIG. 8. Determination of the mean SH frequency $f_{\text{shift}}(t)$ (black down-pointing triangle) on day 18 of the long-term measurement. Four SHs ($j = 1$ to 4, blue squares) were scanned once with decreasing frequency and another set ($j = 5$ to 8, red circles) was scanned once with increasing AOM frequency. The mean value of the "decreasing" scans $\langle \Delta f_{\text{SH},j} \rangle_{\text{dec}}$ is shown as a cyan up-pointing triangle, and the mean value of the "increasing" scans $\langle \Delta f_{\text{SH},j} \rangle_{\text{inc}}$ is shown as a purple diamond.

days. This value is consistent with that of Könz *et al.* [24] who measured a value $\simeq 23$ days at 2 K for site 1.

B. Long-term frequency drift

A systematic frequency shift occurs when determining the SH center frequency: the latter depends on the sign of the
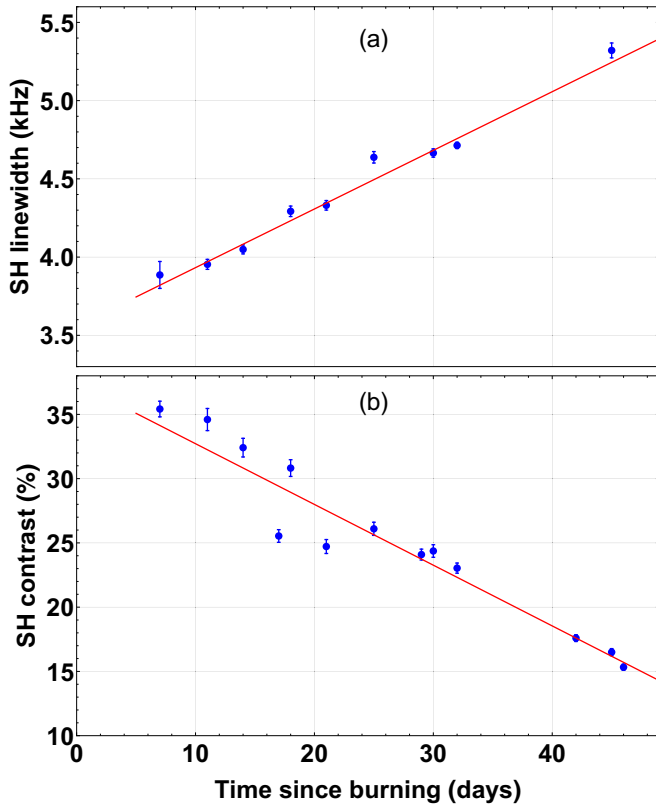
frequency steps introduced by the AOM during the line scan. We measured this effect precisely for the abovementioned settings by burning 20 SHs within 2 min and scanning them 2 to 18 min later. One half of the SHs was scanned by increasing f_{AOM}; the other half was scanned in reverse. We measured a difference of 298(47) Hz between the average center frequencies $\langle \Delta f_{\text{SH},j} \rangle$ of the two subsets. Therefore, in our long-term measurements, we determined the frequency shifts as follows. At a particular (nominal) time t, we measured, within approximately half an hour, the mean SH center frequency $\langle \Delta f_{\text{SH},j} \rangle_{\text{inc}}$ of a set of at least 4 SHs scanned with rising AOM frequency and the mean frequency $\langle \Delta f_{\text{SH},j} \rangle_{\text{dec}}$ of another set of at least 4 SHs with falling frequency. The average frequency shift $f_{\text{shift}}(t)$ of the SHs at time t is defined as the mean of $\langle \Delta f_{\text{SH},j} \rangle_{\text{dec}}$ and $\langle \Delta f_{\text{SH},j} \rangle_{\text{inc}}$. An example of such a determination is shown in Fig. 8.

The complete measurement lasting 2 weeks is shown in Fig. 10. A linear fit of the data shows a fractional SH frequency drift of $1.3(10) \times 10^{-19}$/s, where the uncertainty is statistical. This is consistent with a vanishing drift rate. The statistical uncertainty originates from the three contributions already discussed in Sec. IV A, which resulted in $\sigma_{\text{shift}} \simeq 90$ Hz for an individual measurement $\Delta f_{\text{SH},j}$.

A systematic effect is a frequency shift due to long-term temperature drift. The temperature increased monotonically by 15 mK during the measurement period [see Fig. 10(b)]. Taking into account the measured temperature sensitivity (see Sec. IV) the resulting total SH frequency shift is 10 Hz, which is not negligible. Therefore, the data shown in Fig. 10(a) were corrected for the respective calculated thermal shift.

A further possible systematic error is a drift of our frequency reference, the hydrogen maser. A comparison of its
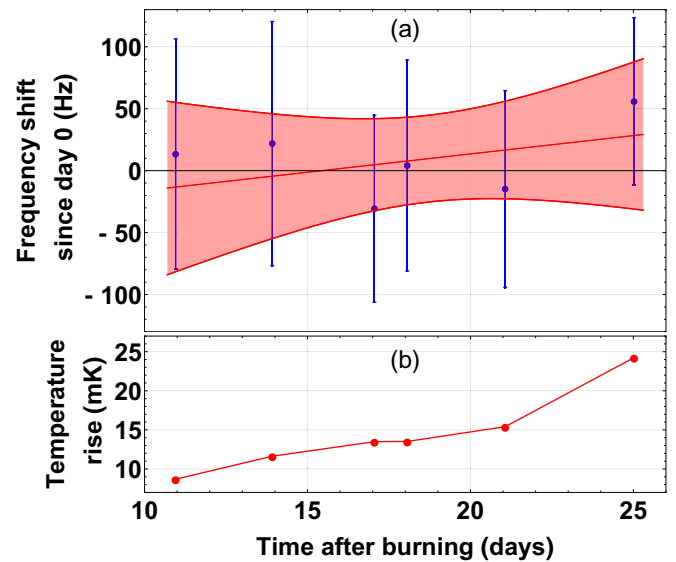

FIG. 9. Long-term variation (a) of the SH linewidth (FWHM) and (b) of the SH contrast C_{h}. Each SH was scanned only once.

FIG. 10. (a) The change in SH frequency, $f_{\text{shift}}(t)$, measured over a period of 14 days. All SHs were burned at time $t = 0$. Red line: linear fit with slope 3(7) Hz/day, or $1.3(10) \times 10^{-19}$ s^{-1} fractionally. The shaded region shows the $\pm 1\sigma$ uncertainty of the fit. (b) Temperature measured at the location of the Eu^{3+} : Y$_2$SiO$_5$ crystal. A calibrated Cernox temperature sensor having a specified accuracy of 5 mK was used.

frequency with the 1 pulse per second signal received from the GPS showed that the maser frequency drift during the measurement period was on the order of 1×10^{-20}/s and can thus be neglected.

VI. SUMMARY AND CONCLUSION

We measured with high frequency resolution and high accuracy the linewidth, the long-term frequency drift, and the temperature-induced frequency shift and line broadening of persistent spectral holes in $Eu^+ : Y_2SiO_5$ at a temperature significantly lower than previously, 1.15 K. Our measurements demonstrated a significant increase of the SH lifetime in comparison to results at 3–4 K [16,19], confirming the estimations [24]. We determined the properties of spectral holes as long as 49 days after burning and found that even at that "age," the holes still exhibited good signal-to-noise ratio and a reasonably small linewidth (5.4 kHz), if previously left undisturbed. No long-term drift of the SH center frequencies over 14 days could be observed, with a 1σ upper limit of 2.3×10^{-19}/s. This is 65 times smaller than the upper limit measured in a previous experiment at 3 K, 1.5×10^{-17}/s [19]. For comparison, cryogenic silicon cavities with drifts as small as 5×10^{-19}/s to 1.4×10^{-20}/s have been reported [26,27]. We expect that it is feasible to reduce the uncertainty of the spectral hole drift by increasing the observation time interval, which in our case was limited because of cryostat performance. A measurement of the temperature-induced hole line shift over the range 1.2–4.1 K accurately confirmed the predicted variation with the fourth power of the temperature. No hysteresis in the hole frequency was found within the measurement error after heating the crystal from 1.15 to 4.1 K and cooling back to 1.15 K.

The long-term properties of spectral holes in this particular system do appear to make it suitable as a long-term-stable frequency reference. In particular, it is favorable that at 1.15 K the temperature sensitivity is only $\simeq 1 \times 10^{-12}$/K fractionally. This is comparable to the lowest values achieved with cryogenic silicon cavities [27]. If required for achieving the most demanding performance, an active temperature stabilization of the host crystal to the microkelvin level could be implemented [19] and this could reduce the effects of temperature instability to the 10^{-18} level.

The SH linewidth observed in this work is also comparable to that of silicon cavities [27]. The signal-to-noise ratio of the spectral hole signals is, of course, significantly lower than that for a cavity. It could be increased, e.g., by using longer crystals, interrogating several crystals in parallel, and increasing the europium concentration.

[1] A. Derevianko and H. Katori, Rev. Mod. Phys. **83**, 331 (2011).

[2] N. Poli, C. W. Oates, P. Gill, and G. M. Tino, Riv. Nuovo Cimento **36**, 555 (2013).

[3] A. D. Ludlow, M. M. Boyd, J. Ye, E. Peik, and P. O. Schmidt, Rev. Mod. Phys. **87**, 637 (2015).

[4] F.-L. Hong, Meas. Sci. Technol. **28**, 012002 (2017).

[5] T. Kessler, C. Hagemann, C. Grebing, T. Legero, U. Sterr, F. Riehle, M. J. Martin, L. Chen, and J. Ye, Nat. Photonics **6**, 687 (2012).

[6] S. Häfner, S. Falke, C. Grebing, S. Vogt, T. Legero, M. Merimaa, C. Lisdat, and U. Sterr, Opt. Lett. **40**, 2112 (2015).

[7] D. G. Matei, T. Legero, S. Häfner, C. Grebing, R. Weyrich, W. Zhang, L. Sonderhouse, J. M. Robinson, J. Ye, F. Riehle, and U. Sterr, Phys. Rev. Lett. **118**, 263202 (2017).

[8] D. Meiser, J. Ye, D. R. Carlson, and M. J. Holland, Phys. Rev. Lett. **102**, 163601 (2009).

[9] R. M. Macfarlane and R. M. Shelby, in *Spectroscopy of Crystals Containing Rare Earth Ions*, Vol. 21 (North-Holland, Amsterdam, 1987), Chap. 3.

[10] M. J. Sellars, R. S. Meltzer, P. T. H. Fisk, and N. B. Manson, J. Opt. Soc. Am. B **11**, 1468 (1994).

[11] P. B. Sellin, N. M. Strickland, J. L. Carlsten, and R. L. Cone, Opt. Lett. **24**, 1038 (1999).

[12] P. B. Sellin, N. M. Strickland, T. Böttger, J. L. Carlsten, and R. L. Cone, Phys. Rev. B **63**, 155111 (2001).

[13] G. J. Pryde, T. Böttger, R. L. Cone, and R. C. C. Ward, J. Lumin. **98**, 309 (2002).

[14] B. Julsgaard, A. Walther, S. Kröll, and L. Rippe, Opt. Express **15**, 11444 (2007).

[15] M. Thorpe, L. Rippe, T. Fortier, M. Kirchner, and T. Rosenband, Nat. Photonics **5**, 688 (2011).

[16] S. Cook, T. Rosenband, and D. R. Leibrandt, Phys. Rev. Lett. **114**, 253902 (2015).

[17] O. Gobron, K. Jung, N. Galland, K. Predehl, R. L. Targat, A. Ferrier, P. Goldner, S. Seidelin, and Y. L. Coq, Opt. Express **25**, 15539 (2017).

[18] M. J. Thorpe, D. R. Leibrandt, and T. Rosenband, New J. Phys. **15**, 033006 (2013).

[19] Q.-F. Chen, A. Troshyn, I. Ernsting, S. Kayser, S. Vasilyev, A. Nevsky, and S. Schiller, Phys. Rev. Lett. **107**, 223202 (2011).

[20] D. R. Leibrandt, M. J. Thorpe, C.-W. Chou, T. M. Fortier, S. A. Diddams, and T. Rosenband, Phys. Rev. Lett. **111**, 237402 (2013).

[21] S. Vogt, C. Lisdat, T. Legero, U. Sterr, I. Ernsting, A. Nevsky, and S. Schiller, Appl. Phys. B **104**, 741 (2011).

[22] R. Yano, M. Mitsunaga, and N. Uesugi, Opt. Lett. **16**, 1884 (1991).

[23] R. W. Equall, Y. Sun, R. L. Cone, and R. M. Macfarlane, Phys. Rev. Lett. **72**, 2179 (1994).

[24] F. Könz, Y. Sun, C. W. Thiel, R. L. Cone, R. W. Equall, R. L. Hutcheson, and R. M. Macfarlane, Phys. Rev. B **68**, 085109 (2003).

[25] D. E. McCumber and M. D. Sturge, J. Appl. Phys. **34**, 1682 (1963).

[26] C. Hagemann, C. Grebing, C. Lisdat, S. Falke, T. Legero, U. Sterr, F. Riehle, M. J. Martin, and J. Ye, Opt. Lett. **39**, 5102 (2014).

[27] E. Wiens, A. Yu. Nevsky, and S. Schiller, Phys. Rev. Lett. **117**, 271102 (2016).